

DESCRIPTION OF THE $\pi^+\pi^-$ PHOTOPRODUCTION*

NADINE HAMMOUD

for the JPAC Collaboration

Institute of Nuclear Physics Polish Academy of Sciences, Kraków, Poland

*Received 27 December 2022, accepted 23 September 2023,
published online 27 October 2023*

Photoproduction is well-known as an excellent technique for studying nucleon resonances, particularly exotic meson states. Our focus centers on the $\gamma p \rightarrow \pi^+\pi^-p$ reaction with the aim of investigating the interference of meson resonance generation and meson–baryon rescattering effects. The Deck model is employed to characterize the basic aspects of diffractive $\pi^+\pi^-$ photoproduction, assuming that virtual pion (denoted as π^*) exchange is dominant. In an effort to describe the most recent data obtained from the CLAS12 and GlueX investigations and to validate the theoretical model, the moments of angular distributions and the projected mass distribution of P -wave are computed in the helicity frame, which is the rest frame of the $\pi\pi$ system with its direction opposite to the z -axis.

DOI:10.5506/APhysPolBSupp.16.8-A5

1. Introduction

It is widely recognized that QCD predicts the existence of unconventional meson states that carry quantum numbers which are not accessible in the $q\bar{q}$ systems like 0^{+-} , 1^{-+} , 2^{+-} . The occurrence of such spin-exotic states would be a clear sign of the presence of particles containing more than two quarks or gluonic excitations. A lot of experimental signs of structural diversity have been detected through observations and confirmation of multiquark states at current particle colliders [1–4]; these findings make the next chapter of hadronic physics an exciting prospect as we search for more exotic states, particularly those with explicit gluonic content [5]. Such unconventional hadrons provide a unique insight into the characteristics of the gluon, the mechanism of color confinement, and the strong interaction, making them an essential research subject while the photoproduction process appears to be a favorable source for the creation of exotic mesons due to the abundance of experimental data of the double pion photoproduction. In the next sections, we shall present a full investigation of the $\pi^+\pi^-$ photoproduction.

* Presented at *Excited QCD 2022*, Sicily, Italy, 23–29 October, 2022.

2. Model description

The main characteristics of diffractive $\pi^+\pi^-$ photoproduction may be interpreted as the outcome of two competing processes, which we will call the continuum and resonant components, respectively (see Fig. 1). The continuous contribution is described in this model as originating from diffractive scattering of the photon on the target nucleon. We believe that one-pion exchange will dominate due to the long-term nature of the connection. This is referred to as the Deck mechanism [6]. We shall use the following invariants in our study:

$$s = (p_1 + q)^2 = (p_2 + k_1 + k_2)^2, \quad (1)$$

$$t = (p_1 - p_2)^2 = (k_1 + k_2 - q)^2, \quad (2)$$

$$u = (q - p_2)^2 = (p_1 - k_1 - k_2)^2, \quad (3)$$

$$s_1 = (p_2 + k_1)^2, \quad t_1 = (p_1 - k_1)^2, \quad (4)$$

$$u_1 = (q - k_1)^2 = (p_1 - k_2 - p_2)^2, \quad (5)$$

$$s_2 = (p_2 + k_2)^2, \quad t_2 = (p_1 - k_2)^2, \quad (6)$$

$$u_2 = (q - k_2)^2 = (p_1 - k_1 - p_2)^2, \quad (7)$$

$$s_{\pi\pi} = (k_1 + k_2)^2 = (p_1 - p_2 + q)^2, \quad (8)$$

where s is the total c.m. energy squared, t is the total four-momentum transfer, $s_{\pi\pi}$ is the invariant mass of the $\pi\pi$ system squared. s_1, t_1, u_1 and s_2, t_2, u_2 are the invariants corresponding to $\pi^{*+}N \rightarrow \pi^+N$ and $\pi^{*-}N \rightarrow \pi^-N$ scattering processes respectively.

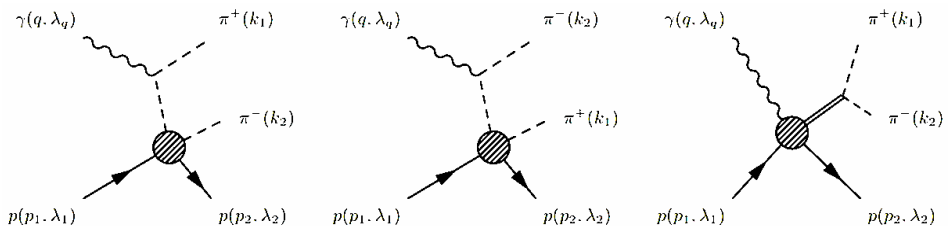


Fig. 1. The Deck mechanism for two pion photoproduction. Note that either charged pion may couple with the incoming photon.

2.1. Deck model

The gauge-invariant Deck amplitude [6, 8] is defined as

$$\begin{aligned} & \mathcal{M}_{\lambda_1\lambda_2\lambda_q}^{\text{Deck,GI}}(s, t, s_{12}, \Omega) \\ &= \sqrt{4\pi\alpha} \left[\left(\frac{\epsilon(q, \lambda_q) \cdot k_1}{q \cdot k_1} - \frac{\epsilon(q, \lambda_q) \cdot (p_1 + p_2)}{q \cdot (p_1 + p_2)} \right) \beta(t_{\pi_1}) \mathcal{M}_{\lambda_1\lambda_2}^-(s_2, t; t_{\pi_1}) \right. \\ & \quad \left. - \left(\frac{\epsilon(q, \lambda_q) \cdot k_2}{q \cdot k_2} - \frac{\epsilon(q, \lambda_q) \cdot (p_1 + p_2)}{q \cdot (p_1 + p_2)} \right) \beta(t_{\pi_2}) \mathcal{M}_{\lambda_1\lambda_2}^+(s_1, t; t_{\pi_2}) \right], \quad (9) \end{aligned}$$

where $\mathcal{M}_{\lambda_1\lambda_2}^\pm$ represents the scattering amplitude for the $p + \pi^{*\pm} \rightarrow p + \pi^\pm$ process, and $\beta(t_i) = \exp((t_i - t_i^{\min})/\Lambda_\pi^2)$ are the hadronic form factors that were introduced to suppress the Born term pion propagator for the one-pion exchange at large t_i , where $\Lambda_\pi = 0.9$ GeV. We define the minimum pion virtuality t_i^{\min} as

$$t_{\pi_1}^{\min} = m_\pi^2 - \frac{1}{2s} \left[(s - m_N^2)(s - s_2 + m_\pi^2) - \lambda^{1/2}(s, 0, m_N^2) \lambda^{1/2}(s, s_2, m_\pi^2) \right], \quad (10)$$

$$t_{\pi_2}^{\min} = m_\pi^2 - \frac{1}{2s} \left[(s - m_N^2) * (s - s_1 + m_\pi^2) - \lambda^{1/2}(s, 0, m_N^2) \lambda^{1/2}(s, s_1, m_\pi^2) \right]. \quad (11)$$

2.1.1. Pion–proton scattering

The scattering amplitude of $\pi^{\pm*}p$ process may be written as

$$T_\lambda^+ = \bar{u}_\lambda(p_2) \left[A^+ + \frac{1}{2} \gamma_\mu (q - k_2 + k_1)^\mu B^+ \right] u_\lambda(p_1), \quad (12)$$

$$T_\lambda^- = \bar{u}_\lambda(p_2) \left[A^- + \frac{1}{2} \gamma_\mu (q - k_1 + k_2)^\mu B^- \right] u_\lambda(p_1), \quad (13)$$

where A and B are scalar functions in the nucleon resonance region which can be parametrized using a partial wave expansion as follows:

$$\frac{1}{4\pi} A = \frac{\sqrt{s} + m_p}{Z_1^+ Z_2^+} f_1 - \frac{\sqrt{s} - m_p}{Z_1^- Z_2^-} f_2, \quad (14)$$

$$\frac{1}{4\pi} B = \frac{1}{Z_1^+ Z_2^+} f_1 - \frac{1}{Z_1^- Z_2^-} f_2, \quad (15)$$

where f_1 and f_2 are called the reduced helicity amplitudes, E_i are the nucleon momenta and $Z_i^\pm = \sqrt{E_i^{\text{CM}} \pm m_p}$. The partial wave decomposition can be

written as

$$f_1 = \frac{1}{\sqrt{|\mathbf{p}_1^{\text{CM}}| |\mathbf{p}_2^{\text{CM}}|}} \sum_{l=0}^{\infty} f_{l+}(s) P'_{l+1}(z) - \frac{1}{\sqrt{|\mathbf{p}_1^{\text{CM}}| |\mathbf{p}_2^{\text{CM}}|}} \sum_{l=2}^{\infty} f_{l-}(s) P'_{l-1}(z), \quad (16)$$

$$f_2 = \frac{1}{\sqrt{|\mathbf{p}_1^{\text{CM}}| |\mathbf{p}_2^{\text{CM}}|}} \sum_{l=1}^{\infty} [f_{l-}(s) - f_{l+}(s)] P'_l(z), \quad (17)$$

where $P'_l(z) = \frac{d}{dz} P_l(z)$ are the first derivatives of the Legendre polynomials, and $z = \cos(\theta_s)$. It is noteworthy that A and B amplitudes depend on the pion virtuality $t_\pi = (q - k_i)^2$ which appears clearly in the scattering angle expression

$$\cos(\theta_s) = \frac{2s_i (t - 2m_p^2) + (s_i - t_{\pi i} + m_p^2) (s_i - m_\pi^2 + m_p^2)}{\sqrt{\lambda(s_i, t_{\pi i}, m_p^2)} \sqrt{\lambda(s_i, m_\pi^2, m_p^2)}}. \quad (18)$$

3. Helicity frame

We are focused on the kinematics within the helicity frame, in which the negative z -axis is determined by the direction of the recoiling proton (p_2). In this context, our momentum vectors can be expressed as follows:

$$\mathbf{p}_1^H = |\vec{p}_1|(\sin \theta_1, 0, \cos \theta_1), \quad (19)$$

$$\mathbf{p}_2^H = |\vec{p}_2|(0, 0, -1), \quad (20)$$

$$\mathbf{k}_1^H = \left| \vec{k}_1 \right| (\sin \theta \cos \phi, \sin \theta \sin \phi, \cos \theta) = -\vec{k}_2^H, \quad (21)$$

$$\mathbf{q}^H = |\vec{q}|(-\sin \theta_q, 0, \cos \theta_q). \quad (22)$$

This allows one to compute the energies of the particles in this frame

$$E_1 = \frac{s + t - m_p^2}{2\sqrt{s_{\pi\pi}}}, \quad (23)$$

$$E_2 = \frac{s - s_{\pi\pi} - m_p^2}{2\sqrt{s_{\pi\pi}}}, \quad (24)$$

$$E_q = q = \frac{s_{\pi\pi} - t}{2\sqrt{s_{\pi\pi}}}, \quad (25)$$

$$E_{k_1} = E_{k_2} = \frac{\sqrt{s_{\pi\pi}}}{2}. \quad (26)$$

4. Resonance production

The production process of the $\rho(770)$ resonance is primarily governed by both the Pomeron (\mathbb{P}) and f_2 exchanges. The general amplitude can be expressed as follows:

$$\begin{aligned}\mathcal{M}_{\lambda,\lambda_1,\lambda_2}^{\mathbb{N}} &= \frac{-1}{s} g_{\rho\pi} \beta_{\mathbb{N}}^{\gamma\rho} \text{BW}(s) R(s, t) \bar{u}(p_2, \lambda_2) \gamma^\mu u(p_1, \lambda_1) \nu_\mu^\lambda \times e^{\beta_{\mathbb{N}} t} \\ &= M_{\mathbb{N}} e^{\beta_{\mathbb{N}} t},\end{aligned}\quad (27)$$

where (\mathbb{N}) represents the Natural Reggeon exchange that is either \mathbb{P} or f_2 exchanges

$$R(s, t) = \frac{\alpha_{\mathbb{N}}(t)}{\alpha_{\mathbb{N}}(0)} \frac{1 + e^{i\pi\alpha_{\mathbb{N}}(t)}}{\sin(\pi\alpha_{\mathbb{N}}(t))} \left(\frac{s}{s_0}\right)^{\alpha_{\mathbb{N}}(t)} \quad (28)$$

with the following linear trajectories for both the Pomeron and f_2 exchanges:

$$\alpha_{\mathbb{P}}(t) = 1.08 + 0.25t, \quad (29)$$

$$\alpha_{f_2}(t) = 0.5 + 0.9t. \quad (30)$$

We use the energy-dependent distribution

$$\text{BW}(s) = \frac{1}{m_\rho^2 - m_{\pi\pi}^2 - im_\rho \Gamma(s)} \quad \text{with} \quad \Gamma(s) = \left(\frac{s - 4m_\pi^2}{m_\rho^2 - 4m_\pi^2}\right)^{3/2}. \quad (31)$$

To achieve better agreement with the CLAS data and the data presented in [7], we made efforts to adjust the t dependency of our model by introducing two additional parameters in the amplitude through the f_2 exchange. Consequently, the total P -wave amplitude is defined as follows:

$$\mathcal{M}_{\lambda,\lambda_1,\lambda_2} = M_{\mathbb{P}} e^{\beta_P t} + M_{f_2} \left((1 - \epsilon) e^{\beta_{f_2}^1 t} + \epsilon e^{\beta_{f_2}^2 t} \right). \quad (32)$$

The constants are:

$$\begin{aligned}g_{\rho\pi} &= 5.96, & \beta_P^{\gamma\rho} &= 2.506, & \beta_P &= 3.6, & \beta_{f_2}^{\gamma\rho} &= 2.47, \\ \beta_{f_2}^1 &= 0.55, & \beta_{f_2}^2 &= -0.20923732, & \epsilon &= 1.3710881, & s_0 &= 1 \text{ GeV}^2.\end{aligned}\quad (33)$$

5. Cross section and moments

After describing the model's major theoretical components, we now validate it by comparing predictions to measurements of two-pion photoproduction produced by the CLAS Collaboration [10]. The differential cross

section can be expressed as

$$\frac{d\sigma}{dt dm_{\pi\pi} d\Omega} = \frac{1}{2}(2\pi)\kappa \sum_{\lambda_q \lambda_1 \lambda_2} \left| \sum_{L=0}^{\infty} \sum_{M=-L}^L \mathcal{M}_{\lambda_1 \lambda_2 \lambda_q}^{LM}(s, t, s_{\pi\pi}) Y_{LM}(\Omega) \right|^2. \quad (34)$$

Projecting the P -wave on Eq. (34) gives

$$\frac{d\sigma_L}{dt} = \sum_{M=-L}^L \int_{m_{\pi\pi}^{\min}}^{m_{\pi\pi}^{\max}} dm_{\pi\pi} \frac{1}{2}(2\pi)\kappa \sum_{\lambda_q \lambda_1 \lambda_2} \left| \mathcal{M}_{\lambda_1 \lambda_2 \lambda_q}^{LM}(s, t, s_{\pi\pi}) \right|^2 \quad (35)$$

with κ being the phase factor *i.e.*

$$\kappa = \frac{1}{(2\pi)^3} \frac{1}{4\pi} \frac{1}{2\pi} \frac{\lambda^{1/2}(s_{\pi\pi}, m_{\pi}^2, m_{\pi}^2)}{16\sqrt{s_{\pi\pi}}(s - m_p^2)^2} \frac{1}{2}. \quad (36)$$

In order to compute the moments we follow the conventions given in Ref. [10], that is

$$\langle Y_{LM} \rangle(s, t, m_{\pi\pi}) = \sqrt{4\pi} \int d\Omega \frac{d\sigma}{dt dm_{\pi\pi} d\Omega} \text{Re} Y_{LM}(\Omega). \quad (37)$$

This normalization ensures that

$$\langle Y_{00} \rangle(s, t, m_{\pi\pi}) = \frac{d\sigma}{dt dm_{\pi\pi}}. \quad (38)$$

Another convention was discussed in [9] where one can convert it into the moments defined by CLAS [10] using

$$\langle Y_{LM} \rangle = (2\pi)\sqrt{2L+1}H^0(LM). \quad (39)$$

Remark: $d_{M0}^L(\theta)$ computed with DDJMNB from CERLIB.

6. Results

Figure 2 presents our predicted P -wave mass distributions, which are compared with the CLAS measurements spanning the mass range of $m_{\pi\pi} \in [0.4, 1.2]$ GeV at a beam energy of $E_\gamma = 3.4$ GeV². The enhancements made to our model are clearly reflected in the improved agreement with the experimental data obtained by CLAS. Additionally, we have computed the moments of angular distributions at two distinct beam energies and various momentum transfers for comparison with both the CLAS ($E_\gamma = 3.4$ GeV²) and Ballam ($E_\gamma = 4.7$ GeV²) data, as illustrated in Fig. 3. Here, s_{12} represents the square of the $\pi\pi$ energy, denoted as $s_{\pi\pi}$. Upon scrutiny of the results presented in Fig. 3, it becomes evident that our model effectively describes the $\langle Y_{00} \rangle$ data across different t values.

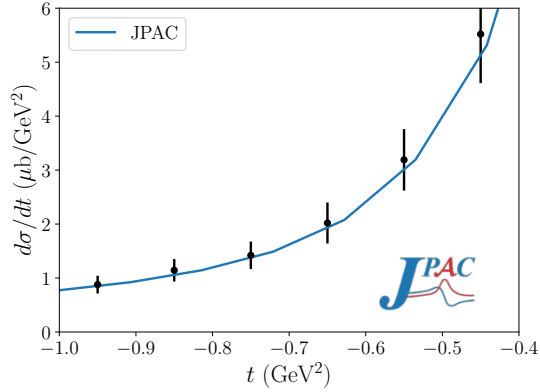


Fig. 2. Comparison between our predicted P -wave mass distributions and the data obtained.

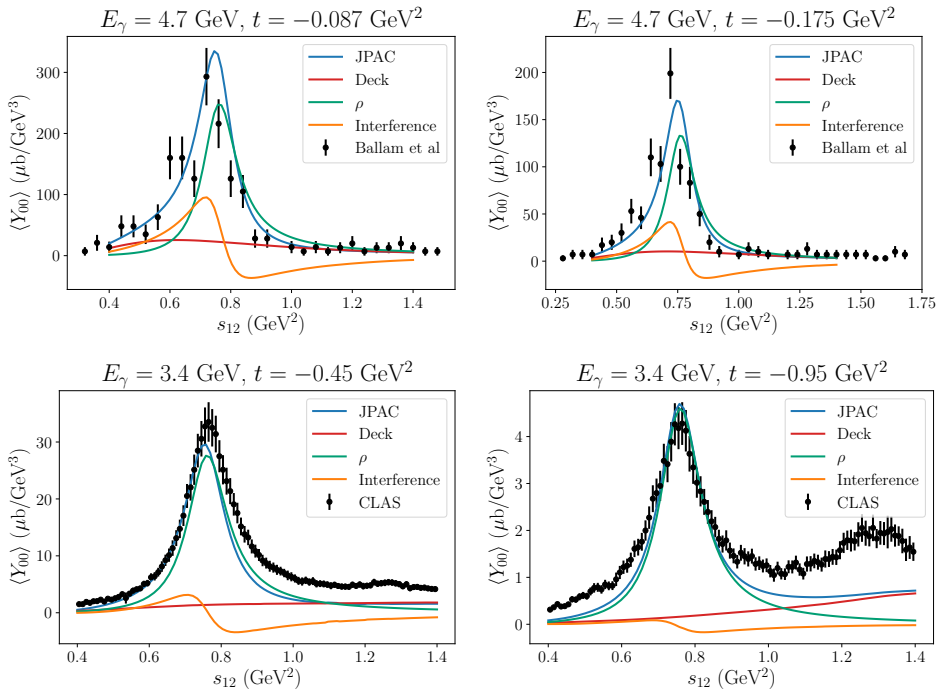


Fig. 3. Comparing the prediction of JPAC model with experimental data from the Ballam (upper plots) and CLAS data (lower plots).

7. Summary

We have described the model used in studying double-pion photoproduction process and computed both the mass distribution and the moments of $\pi^+\pi^-$ angular distributions for different beam energies and momentum transfer.

The presented work has been done in collaboration with the JPAC group *i.e.* Adam Szczepaniak, Łukasz Bibrzycki, Vincent Mathieu, and R.J. Perry. This work was partly financed by the National Science Center (NCN), Poland, project No. 2018/29/B/ST2/02576 as well.

REFERENCES

- [1] BESIII Collaboration (M. Ablikim *et al.*), *Phys. Rev. Lett.* **110**, 252001 (2013).
- [2] Belle Collaboration (Z.Q. Liu *et al.*), *Phys. Rev. Lett.* **110**, 252002 (2013).
- [3] LHCb Collaboration (R. Aaij *et al.*), *Phys. Rev. Lett.* **115**, 072001 (2015).
- [4] LHCb Collaboration (R. Aaij *et al.*), *Phys. Rev. Lett.* **117**, 152003 (2016).
- [5] GlueX Collaboration (H. Al Ghoul *et al.*), *AIP Conf. Proc.* **1735**, 020001 (2016).
- [6] R.T. Deck, *Phys. Rev. Lett.* **13**, 169 (1964).
- [7] J. Ballam *et al.*, *Phys. Rev. D* **5**, 545 (1972).
- [8] J. Pumplin, *Phys. Rev. D* **2**, 1859 (1970).
- [9] JPAC Collaboration (V. Mathieu *et al.*), *Phys. Rev. D* **100**, 054017 (2019), [arXiv:1906.04841](https://arxiv.org/abs/1906.04841) [hep-ph].
- [10] CLAS Collaboration (M. Battaglieri *et al.*), *Phys. Rev. D* **80**, 072005 (2009), [arXiv:0907.1021](https://arxiv.org/abs/0907.1021) [hep-ex].